J|A|C|S
COMMUNICATIONS

Published on Web 05/10/2005

Controlling Interparticle Spacing among Metal Nanoparticles through Metal-Catalyzed Decomposition of Surrounding Polymer Matrix

Kensuke Akamatsu,*[,†,‡] Hiroyuki Shinkai,[‡] Shingo Ikeda,[‡] Satoshi Adachi,[†] Hidemi Nawafune,*[,†,‡] and Satoshi Tomita[§]

Faculty of Science and Engineering and Graduate School of Science, Konan University, 8-9-1 Okamoto, Higashinada, Kobe 658-8501, Japan, and PRESTO, Japan Science and Technology Agency (JST), Wako, Saitama 351-0198, Japan

Received February 4, 2005; E-mail: akamatsu@center.konan-u.ac.jp

Nanocomposites containing inorganic nanoparticles have been of great interest in recent years due to their potential application for novel electronic, optical, and magnetic devices.[1] The size of the nanoparticles is one of the key parameters that determine the properties of the nanocomposites. Additionally, physical interactions among nanoparticles, such as electric and magnetic dipole interactions, are recognized to be important in the next generation nanodevices, including plasmon waveguides,[2] biosensors,[3] and ultrahigh density data storage media.[4] Since the physical interactions depend on both the particle size and interparticle spacing, precise control over the spacing under a fixed particle size is an important challenge for understanding the physical interactions in the nanocomposite systems. However, previous attempts at control over microstructures of the nanocomposites did not enable one to independently control the interparticle spacing and the nanoparticle size.[5]

Herein, we report a novel method to control the average interparticle spacing among metal nanoparticles embedded in a polyimide matrix based on an in situ approach using ion-doped precursors.[6,7] This is achieved by the metal-catalyzed decomposition of the surrounding matrix, which induces a decrease in thickness (i.e., volume) of the composite layer, while the nanoparticle size remains intact (Figure 1A). This holds great promise not only toward the fundamental understanding of the physical interactions among metal nanoparticles but also toward the development of novel nanocomposites with tailored microstructures.

The approach works by the hydrolysis of polyimide resin using an alkali solution, subsequent incorporation of metal ions through ion exchange, followed by hydrogen-induced reduction of ions to form metal nanoparticles. In a typical procedure, the PMDA-ODA-type polyimide films were treated with aqueous KOH solution (5 M at 50 °C) for 5 min to form layers of potassium salts of poly(amic acid)[6,8] with a thickness of 3 μm. The formed carboxylic acid groups can be used as ion exchange sites for subsequent doping of metal ions using aqueous 10 mM $PtCl_2$ (containing 1 M NH_3), 50 mM $NiCl_2$, or 50 mM $CuSO_4$ solutions, thus generating the ion-doped precursor layers (ion loading: 3.8 ± 0.2 mmol cm^{-3}). Formation of metal nanoparticles was achieved by annealing the precursors at 270−400 °C in a hydrogen atmosphere in a quartz tube.

Metal nanoparticles (4−10 nm in diameter) are generated upon hydrogen reduction, during which the modified layers are again transformed to polyimide through a thermally induced dehydration reaction (re-imidization).[6b] The reduction temperature depends on the metal ions doped into the precursors. For example, 5.4 nm diameter Pt nanoparticles are formed upon 270 °C annealing for 30 min (Figure 1B). Similarly, 7.3 nm Ni and 9.1 nm Cu nanoparticles are formed upon annealing at 290 and 400 °C,

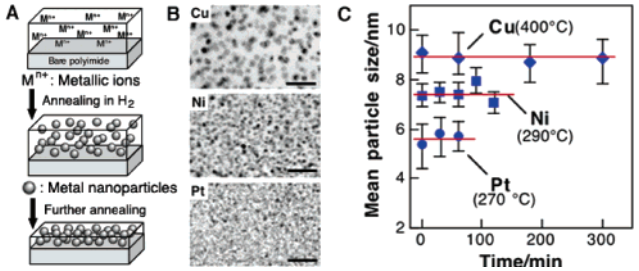

Figure 1. (A) Schematic for controlling the interparticle spacing in the nanocomposites. (B) Cross-sectional TEM images of nanocomposite films containing Pt, Ni, and Cu nanoparticles prepared by annealing in a hydrogen atmosphere at 270 °C (Pt), 290 °C (Ni), and 400 °C (Cu) for 30 min. Scale bar: 50 nm. (C) Changes in nanoparticle size as a function of annealing time. Lines serve as guides to the eyes.

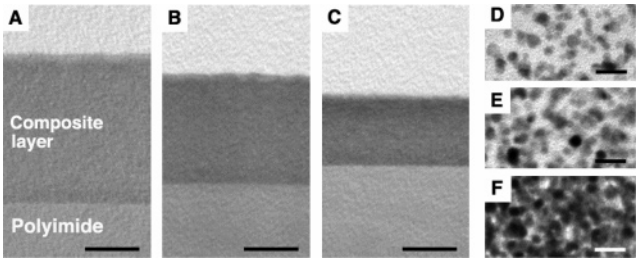

Figure 2. Cross-sectional TEM images of nanocomposite thin films containing Ni nanoparticles. The films were annealed at 290 °C for 30 (A), 60 (B), and 90 min (C). Scale bar: 500 nm. (D−F) High-magnification images of the composite layers corresponding to images (A), (B), and (C), respectively. Scale bar: 20 nm.

respectively.[9] The nanoparticle size remains intact upon longer annealing (Figure 1C). Longer annealing at the fixed temperature, however, causes a decrease in composite layer thickness. Typical examples are shown in Figure 2A−C. The thickness of the composite layer containing Ni nanoparticles decreases from 1.4 to 0.7 μm as the annealing time increases from 30 to 90 min. It is important to note that only the concentration of Ni nanoparticles increases, as can be seen in the TEM images (Figure 2D−F). We confirmed by tilting experiments during TEM observation that anisotropic distribution, concentration gradient of the nanoparticles, and interparticle contact were not observed in the present experimental conditions.

The decrease in layer thickness with fixed nanoparticle size was also observed for Pt and Cu samples, although the rate of decrease in thickness was highly dependent on the species of metals and the temperatures (Figure 3A). In addition, a decrease in film weight upon annealing was observed. The time dependence of the decrease in the layer thickness is quite similar to that of the decrease in film weight (Figure 3B). We also found solid decomposition products on the inner wall of the quartz tube after annealing. It should be

† Faculty of Science and Engineering, Konan University.
‡ Graduate School of Science, Konan University.
§ PRESTO, JST.

10.1021/ja050735+ CCC: $30.25

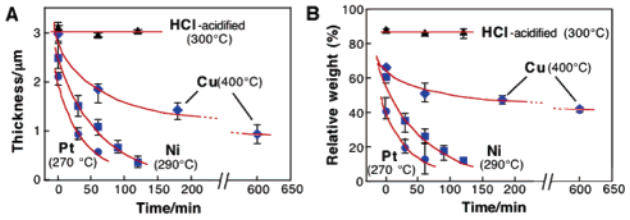

Figure 3. Changes in thickness (A) and weight (B) of the composite layer as a function of annealing time. The weight was normalized to that of film before annealing. The data obtained from the films acidified with HCl (1 vol %) after KOH treatment are also shown. The films were annealed at 270 °C (Pt), 290 °C (Ni), 300 °C (HCl-acidified film), and 400 °C (Cu). Lines serve as guides to the eyes.

noted here that no decrease in layer thickness and weight was observed for acidified films (without metallic ions, Figure 3). These results allow one to conclude that the decrease in film thickness is caused by metal-catalyzed decomposition of polyimide surrounding the metal nanoparticles.

Similar trends have been observed for cellulose fibers containing Pt nanoparticles[10] and polyimide films containing Fe nanoparticles,[11] both of which resulted in the formation of a carbon matrix through carbonization (pyrolysis) of the matrix at high temperatures. Oxidative degradation of thick polyimide films containing Ag nanoparticles was also observed, but resulted in a broad size distribution and inhomogeneous distribution of the nanoparticles in the film.[7b] In the current process, however, a different mechanism for metal-catalyzed decomposition is operative. First, the molecular structure after longer annealing was identified using infrared spectroscopy as the fully cured polyimide (Figure S1), indicating that carbonization of the matrix did not occur. Second, annealing in inert atmosphere did not induce decomposition of the matrix (results not shown). Third, an FTIR spectrum of the decomposition products shows the weak vibrational bands characteristic of NH_2 and CHO splits in addition to strong vibrational bands for polyimide and an amide bond (Figure S2). From these results, although further experiments are necessary to fully elucidate the decomposition mechanism, the current process involves decomposition of the matrix by partial hydrogenation of the imide ring to form the aldehyde and amide bond (imide ring cleavage) and finally the dialdehyde and amine (amide bond cleavage), generating oligomeric (low molecular weight) molecules that are vaporized during annealing. Since the imidized PMDA-ODA matrix is in a glassy state at the present temperature range (T_g = 420 °C)[12] and the catalytic reaction would occur only at the particle/matrix interface, the nanoparticles do not have mobility to come in contact with others so that the nanoparticles are effectively isolated without coalescence.

The gradual decrease in the composite layer thickness, under a fixed nanoparticle size and total number of metal atoms in the film, indicates a gradual increase in the volume faction (f), and thus a gradual decrease in the average interparticle spacing. The f is given by following equation:

$$f = CL_0M_w\rho^{-1}L^{-1} \quad (1)$$

where C, L_0, M_w, ρ, and L are initial ion loading, initial composite layer thickness, atomic weight of metals, density of the metal, and composite layer thickness after annealing, respectively. The average interparticle distance between metal nanoparticles was estimated using f and particle size by assuming that the particles are arranged in a simple cubic lattice. In the present system, the f could be controlled in the range of 5.0−18.3, 4.2−28.1, and 3.5−11.1% for Pt, Ni, and Cu nanoparticles, respectively.[13] These values give average interparticle spacings (surface-to-surface distance) of 6.5−2.4 (Pt), 9.8−4.0 (Ni), and 13.4−6.0 (Cu) nm (longer to shorter limits, obtained by lower to higher volume fractions). The estimated distances become comparable and shorter than the corresponding nanoparticle size, a regime where particle-to-particle interactions are thought to play an important role in determining the physical properties of the resulting nanocomposites. Efforts to explore optical and magnetic properties are currently underway.

This communication describes the systematic control of interparticle spacing among metal nanoparticles embedded in a high-performance polyimide matrix via metal-catalyzed in situ decomposition of the polyimide matrix. The strategy is quite general and extendable to other noble metals and transition metal alloys.[14] The ability to control interparticle spacing with a fixed amount of metal and nanoparticle size enables the elucidation of the effect of particle-to-particle interactions in studies of optical, electrical, and magnetic properties of the nanocomposites. An understanding of these physical properties and their relationship to the material microstructures is essential for initiating new technological applications of metal/polymer nanocomposite materials, especially in the area of optoelectronic and electromagnetic devices.

Acknowledgment. This work was supported in part by JSPS. S.I. is grateful for research fellowship support from JSPS.

Supporting Information Available: Film characterization and FTIR spectra. This material is available free of charge via the Internet at http://pubs.acs.org.

References

(1) (a) MacLachlan, M.; Ginzburg, M.; Coombs, N.; Coyle, T. W.; Raju, N. P.; Greedan, J. E.; Ozin, G. A.; Manners, I. *Science* **2000**, *287*, 1460−1463. (b) Huyuh, W. U.; Dittmer, J. J.; Alivisatos, A. P. *Science* **2002**, *295*, 2425−2427. (c) Coe, S.; Woo, W. K.; Bawendi, M.; Bulovic, V. *Nature* **2002**, *420*, 800−803. (d) Tessler, N.; Medvedev, V.; Kazes, M.; Kan, S.; Banin, U. *Science* **2002**, *295*, 1506−1508. (e) Korchev, A. S.; Bozack, M. J.; Slaten, B. L.; Mills, G. *J. Am. Chem. Soc.* **2004**, *126*, 10−11.

(2) Maier, S. A.; Kik, P. G.; Atwater, H. A.; Meltzer, S.; Harel, E.; Koel, B. E.; Requicha, A. A. G. *Nat. Mater.* **2003**, *2*, 229−232.

(3) (a) Elghanian, R.; Storhoff, J. J.; Mucic, R. C.; Letsinger, R. L.; Mirkin, C. A. *Science* **1997**, *277*, 1078−108. (b) Jin, R.; Wu, G.; Li, Z.; Mirkin, C. A.; Schatz, G. C. *J. Am. Chem. Soc.* **2003**, *125*, 1643−1654.

(4) (a) Sun, S.; Murray, C. B.; Weller, D.; Folks, L.; Moser, A. *Science* **2000**, *287*, 1989−1992. (b) Kleemann, W.; Petracic, O.; Binek C.; Kakazei, G. N.; Pogorelov, Y. G.; Sousa, J. B.; Cardoso, S.; Freitas, P. P. *Phys. Rev. B* **2001**, *63*, 134423−134427. (c) Ebels, U.; Duvail, J. L.; Wigen, P. E.; Piraux, L.; Buda, L. D.; Ounadjela, K. *Phys. Rev. B* **2001**, *64*, 144421−144426.

(5) (a) Laurent, C.; Mauri, D.; Kay, E.; Parkin, S. S. P. *J. Appl. Phys.* **1989**, *65*, 2017−2020. (b) Heilmann, A.; Werner, J.; Schwarzenberg, D.; Henkel, S.; Grosse, P.; Theiss, W. *Thin Solid Films* **1995**, *270*, 103−108. (c) Salz, D.; Lamber, R.; Wark, M.; Baalmann, A.; Jaeger, N. *Phys. Chem. Chem. Phys.* **1999**, *1*, 4447−4451.

(6) (a) Akamatsu, K.; Ikeda, S.; Nawafune, H.; Deki, S. *Chem. Mater.* **2003**, *15*, 2488−2491. (b) Ikeda, S.; Akamatsu, K.; Nawafune, H.; Nishino, T.; Deki, S. *J. Phys. Chem. B* **2004**, *108*, 15599−15607.

(7) (a) Wang, T. C.; Rubner, M. F.; Cohen, R. E. *Chem. Mater.* **2003**, *15*, 299−304. (b) Southward, R. E.; Thompson, D. W. *Chem. Mater.* **2004**, *16*, 1277−1284. (c) Gaddy, G. A.; Locke, E. P.; Miller, M. E.; Broughton, R.; Albrecht-Schmitt, T. E.; Mills, G. *J. Phys. Chem. B* **2004**, *108*, 17378−17383.

(8) Thomas, R. R.; Buchwalter, S. L.; Buchwalter, L. P.; Chao, T. H. *Macromolecules* **1992**, *25*, 4559−4568.

(9) We confirmed by ICP measurement that there remained no ions for annealed samples. During TEM observation, we also analyzed the area between visible nanoparticles by nanobeam EDX and observed that no signals of metals were detected for annealed samples. These results indicate that all of the initially doped metallic ions were incorporated into the nanoparticles.

(10) He, J.; Kunitake, T.; Nakao, A. *Chem. Commun.* **2004**, *4*, 410−411.

(11) Kaburagi, Y.; Toriyama, T.; Yoshida, A.; Wakabayashi, H.; Hishiyama, Y. *J. Mater. Res.* **2001**, *16*, 352−365.

(12) Faupel, F.; Willecke, R.; Thran, A. *Mater. Sci. Eng.* **1998**, *R22*, 1−55.

(13) The values obtained by assuming the hcp and bcc lattice were only slightly larger (1−2 nm) than those obtained by the simple cubic model.

(14) We have extended our process to Ag, Co, and Fe nanoparticles and Ni_xCo_{1-x} and Ni_xFe_{1-x} alloy nanoparticles. Although the temperature at which the decomposition of polyimide occurs depends on the species of metal and alloy, general behavior is similar to that of Pt, Ni, and Cu.

JA050735+